JOURNAL OF APPLIED ELECTROCHEMISTRY 26 (1996) 249–254

Investigation of the aluminium electrodeposition process in cryolite-based melts using a rotating ring-disc electrode: evidence for the existence of a subvalent intermediate species

R. S. STOJANOVIC, R. DORIN, E. J. FRAZER*

CSIRO Division of Minerals, Institute of Minerals, Energy and Construction, PO Box 124, Port Melbourne, Victoria 3207, Australia

Received 5 April 1995; revised 27 June 1995

The rotating ring-disc electrode technique has been used to investigate the reaction mechanism of the aluminium electrodeposition process in cryolite-based electrolytes. Laboratory studies using high temperature gold-molybdenum and platinum-molybdenum rotating ring-disc electrodes have provided evidence for the existence of a subvalent intermediate species (Al(I)). In a cryolite-alumina electrolyte (bath ratio: 1.5), two well separated convective-diffusion controlled oxidation processes were observed at both a gold and a platinum ring during aluminium electrodeposition at the disc. On the basis of the data presented, a reaction scheme involving reduction of Al(III) to Al(0) via Al(I), followed by chemical dissolution of Al(0) into the bulk electrolyte was proposed. The loss of current efficiency in aluminium smelting was primarily attributed to the chemical dissolution of Al(0), rather than to the formation of a subvalent intermediate species.

1. Introduction

The aluminium electrodeposition process in the Hall–Heroult cell has been the subject of numerous laboratory studies by electrochemical techniques such as chronopotentiometry, cyclic voltammetry and rotating disc voltammetry (see, for example, [1–12]). In spite of these efforts, there remains doubt about the overall reaction mechanism since the experimental data presented to date provide only circumstantial evidence about the nature of the electrodeposition process. The existence of a subvalent intermediate species has been inferred, but the kinetics of the electron transfer step are apparently so fast that electrochemical detection is not possible within the time-scale of conventional measurements [13]. At ambient temperature, fast transient techniques such as high-speed cyclic voltammetry at ultramicroelectrodes can often be used to study rapid electrode reactions [14]. Interestingly, ultramicroelectrodes have recently been described for use in molten carbonates, but to date have been limited to temperatures below 650 °C [15].

The overall mechanism of a metal deposition reaction often contains complex sequences of electrochemical and chemical steps. The applicability of the rotating ring-disc electrode (RRDE) for detection of soluble intermediates in electrochemical reactions is well established [16–18]. Implicit in the RRDE approach (generation of species at one electrode and collection/detection at another) is the assumption that the intermediates have a half-life equal to, or greater than, the average time for convective-diffusional mass transport from the disc to the ring [17]. A notable advantage of the technique is that if the ring is held at constant potential, then the observed currents are free of interferences from double-layer charging. Consequently, the mechanism of a metal deposition reaction can be explored, and the reaction sequence unravelled, in a manner that is not possible with other electrochemical techniques.

Previously we described the development of an RRDE with the thermal, electrochemical and corrosion properties necessary for studies in high temperature fluoride electrolytes [19]. In the present work, the RRDE technique is used to elucidate some fundamental details about the aluminium electrodeposition process in cryolite-based electrolytes. Most importantly, it is shown that under certain conditions it is possible to detect a subvalent intermediate species.

2. Experimental details

A bipotentiostat (Pine Instrument Company, Model AFRDE4) and electrode rotator (Pine Instrument Company, Model AFASRE) were used for all rotating ring-disc measurements; unfortunately, the design of this instrument does not allow for *iR* compensation. Current-voltage traces were recorded on a YEW Type 3086 X–Y recorder (Yokogawa Hokushin Electric, Japan). A graphite electrochemical cell was supported within an Inconel 600 furnace tube and

* Author to whom correspondence should be addressed.

0021-891X

heated by a 4 kW furnace (A. J. Wilcock Scientific & Engineering Equipment, model 5V–4T) equipped with temperature control and programmer units. A continuous stream of argon was passed through the furnace tube and over the electrochemical cell to minimize oxidation of the graphite cell components.

Electrochemical measurements were performed using a standard three-electrode arrangement consisting of either a Au-Mo or Pt-Mo RRDE as the working electrode, the graphite cell as the counter electrode, and an aluminium/cryolite reference electrode ('wetted molybdenum hook' design) [20] containing the same composition as the bulk melt. The RRDE was situated ~ 1 cm below the surface of the melt and ~ 3 cm from the bottom of the graphite crucible. The reference electrode was located immediately adjacent to the RRDE with the tip ~ 2 cm from the RRDE surface.

The design and construction of a high temperature Au–Mo RRDE have been described previously [19]. A preliminary investigation of the performance of various high temperature Au–Mo RRDEs suggested that an electrode with a nominal collection efficiency (N) in the range $0.25 < N < 0.41$ should be suitable for investigations in molten fluoride electrolytes. Generally, the construction of Pt–Mo RRDEs was found to be more difficult than Au–Mo RRDEs because platinum is less malleable than gold, and consequently insulator cracking and ring-disc misalignment were more prevalent during heat-up. This latter problem of noncoplanarity leads to poorly defined and irreproducible voltammograms.

The majority of work was performed using a Au–Mo RRDE with dimensions: disc radius, $r_1 = 0.50$ cm; ring inner radius, $r_2 = 0.54$ cm; ring outer radius, $r_3 = 0.64$ cm; disc area $= 0.79\,cm^2$; and ring area $= 0.37\,cm^2$. The theoretical collection efficiency of an RRDE with these dimensions is 31.70% [17]. The dimensions of the Pt–Mo RRDE were: disc radius, $r_1 = 0.40$ cm; ring inner radius, $r_2 = 0.44$ cm; ring outer radius, $r_3 = 0.53$ cm; disc area $= 0.50\,cm^2$; and ring area $= 0.27\,cm^2$, giving a theoretical collection efficiency of 32.95% [17]. The working range of the gold ring was limited to between 0.7 and 1.6 V by alloy formation and the commencement of anodic process(es), respectively; similarly, the platinum ring was limited to between 0.9 and 1.5 V.

Synthetic cryolite and alumina (courtesy of the Comalco Research Centre, Melbourne, Australia), aluminium fluoride (99.9% CERAC Inc.) and calcium fluoride (99.9% Aldrich Chemical Co. Inc.) were vacuum dried at 120 °C for 4 h and then stored *in vacuo* until required. The various electrolyte components (~ 450 g) were premixed prior to being introduced into the graphite cell. Electrochemical measurements were conducted using electrolytes with bath ratios (BR = wt NaF/wt AlF_3) between 1.5 and 0.75, and at working temperatures 10–20 °C above the melt liquidus.

Elemental analysis of an electrode section, after electrolysis, was carried out on a Jeol JSM-25SIII scanning electron microscope coupled to a Link System X-ray analyser (25 kV accelerator voltage). Prior to analysis, the electrode samples were set into cylinders of epoxy resin and cut perpendicular to their principal axes. The exposed faces were then polished mechanically to a 0.5 μm diamond finish.

3. Results and discussion

3.1. *Proposed mechanism for the aluminium electrodeposition process*

Figure 1 shows typical current–voltage curves obtained at a Au–Mo RRDE in an electrolyte consisting of 90 wt % cryolite and 10 wt % alumina ($BR = 1.5$) at 975 °C, as a result of scanning the disc potential in the negative direction while maintaining the ring potential at 1.2 V. The ring and disc traces show the respective current responses at both a *stationary* (curves (a)) and a rotating (curves (b)) electrode. In both cases, the disc current–disc potential curves were characterized by a large single cathodic wave which was attributed primarily to reduction of Al(III) to Al(0). It is reasonable to assume that the observed anodic ring current at the stationary electrode is due to oxidation of dissolved aluminium (generated at the molybdenum disc, and transported to the ring by natural convection). As expected, the above electrode responses do not provide any explicit details about the nature of the overall reaction mechanism or the possible involvement of a subvalent intermediate species.

Under forced convection, two well-separated oxidation waves were observed at the gold ring, as shown by the ring collection (product detection)

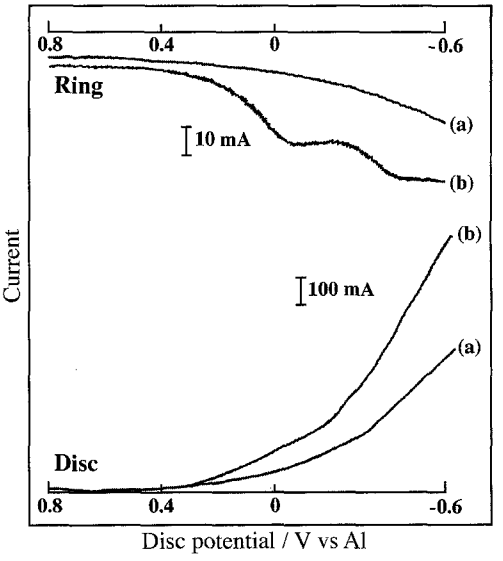

Fig. 1. Typical disc current–disc potential and ring current–disc potential curves obtained at a Au–Mo RRDE ($r_1 = 0.50$ cm, $r_2 = 0.54$ cm, $r_3 = 0.64$ cm, disc area $= 0.79\,cm^2$, and ring area $= 0.37\,cm^2$) in an electrolyte of 90 wt % cryolite and 10 wt % alumina at 975 °C ($BR = 1.5$). (a) Stationary electrode, ring potential 1.2 V and potential scan rate $50\,mV\,s^{-1}$. (b) Rotation rate 1000 r.p.m., ring potential 1.2 V and potential scan rate $50\,mV\,s^{-1}$. (Bottom and top abscissae: disc and ring currents zero, respectively.)

curve. In principle, if the current generated at the disc was totally due to aluminium deposition (assuming there was no dissolution of the product), then the flux of electroactive material reaching the ring, and hence the ring current, would be zero. Therefore, the observed limiting ring currents must have resulted from the convective-diffusion controlled oxidation of soluble species produced at the disc. This behaviour, neglecting possible steps associated with dissociation and competing secondary reactions, suggests that the aluminium electrodeposition process must proceed via an intermediate step as proposed in Scheme I:

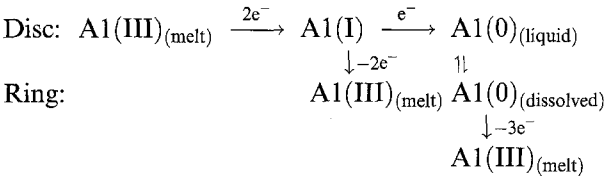

Scheme 1

where Al(III) and Al(I) presumably exist as complex oxyfluoride ions rather than simple ionic species [13]. The data are consistent with a multistep mechanism involving two discrete electron transfer steps, followed by a chemical reaction step involving dissolution of Al(0) into the bulk electrolyte. The proposed mechanism implies that both soluble (Al(I)) and insoluble ($Al(0)_{(liquid)}$) reaction products are formed during the aluminium electrodeposition process. Since aluminium metal is being continuously deposited at the disc as the electrode potential is swept more negative, the ratio of the limiting ring currents cannot be used as a criterion to estimate the number of electrons transferred in the respective oxidation processes.

The instantaneous current efficiency (CE) for a metal electrodeposition reaction, ignoring possible side reactions at the disc, is related to the ratio of the ring and disc currents and can be calculated from the following expression [21]:

$$CE = \left(1 - \frac{i_r}{i_d} \times \frac{1}{N}\right) \times 100 \qquad (1)$$

where i_r = ring current, i_d = disc current and N = collection efficiency of the RRDE. Figure 2 shows a plot of the calculated CE for aluminium electrodeposition versus disc current density using the data of Fig. 1 and N(theoretical) = 31.70%. It is evident from this profile that the CE varies significantly with disc current density, apparently passing through a local maximum ($\sim$ 55% at $\sim 0.1\,A\,cm^{-2}$) and then a local minimum ($\sim$ 43% at $\sim 0.15\,A\,cm^{-2}$), until a limiting value ($\sim$ 86%) is reached. It should be noted that the application of Equation 1 relies on the assumption that the number of electrons transferred at the ring and disc is equal. If the mechanism proceeds via Scheme 1, one would expect the ratio of the electrons being transferred at the ring and disc as the electrode potential is swept more negative to be continuously changing. This may explain the unusual shape of the curve observed in Fig. 2 at lower current densities. Importantly, this curve confirms that even at low current densities aluminium metal is being deposited and partially retained at the disc. This is consistent with the mechanism proposed in Scheme 1, since a proportion of the Al(I) generated at the disc is transported to the ring, while the remainder is reduced and deposited as Al(0). At higher current densities or more negative electrode potentials, the increase in calculated CE is consistent with an increase in the reaction rate of Al(I) to Al(0).

Scheme 1 is a consecutive reaction scheme which does not allow for the possible involvement of two parallel reaction paths, for example, the direct three electron reduction of Al(III) to Al(0). According to Damjanovic *et al.* [22], a plot of the ratio of the disc to the ring currents (i_d/i_r) versus the reciprocal of the square root of rotation rate ($\omega^{-1/2}$) can be used to distinguish between a single path, with or without

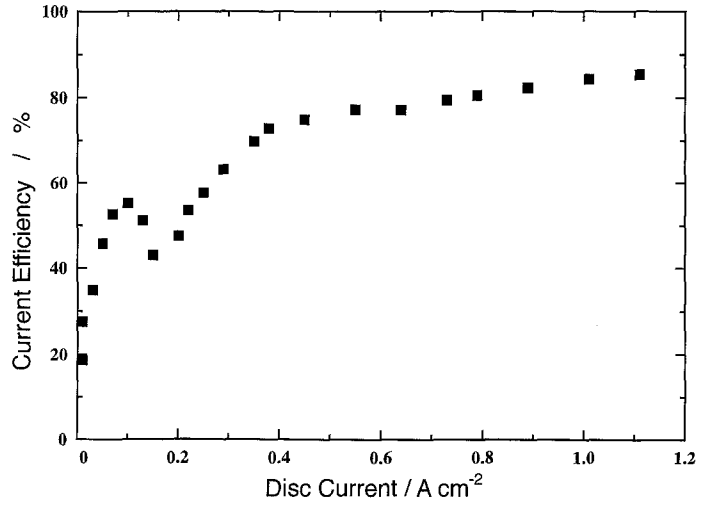

Fig. 2. A plot of calculated current efficiency for aluminium electrodeposition versus disc current density in an electrolyte of 90 wt % cryolite and 10 wt % alumina at 975 °C (BR = 1.5) (data from Fig. 1).

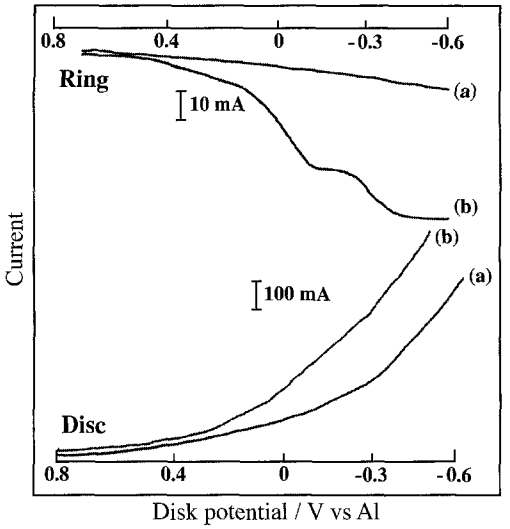

Fig. 3. Typical disc current–disc potential and ring current–disc potential curves obtained at a Pt–Mo RRDE ($r_1 = 0.40$ cm, $r_2 = 0.44$ cm, $r_3 = 0.53$ cm, disc area $= 0.50\,cm^2$, and ring area $= 0.27\,cm^2$) in an electrolyte of 90 wt % cryolite and 10 wt % alumina at 975 °C ($BR = 1.5$). (a) Stationary electrode, ring potential 1.0 V and potential scan rate $50\,mV\,s^{-1}$. (b) Rotation rate: 1000 r.p.m., ring potential 1.0 V and potential scan rate $50\,mV\,s^{-1}$. (Bottom and top abscissae: disc and ring currents zero, respectively.)

an intermediate, and two parallel paths in one of which an intermediate is involved. Unfortunately, the faradaic responses obtained at the Au–Mo RRDE were difficult to measure sufficiently accurately at high rotation rates because of an unfavourable signal to noise ratio. The available data did not fit any of the reaction models suggested by the above authors, so a scheme involving two parallel reactions cannot be discounted. In addition, a plot of the limiting current for each process at the ring (i_r) versus the square-root of rotation rate ($\omega^{1/2}$), did not show the linear dependence usually expected for a simple convective-diffusion controlled system involving only soluble species [17].

Figure 3 shows current-voltage curves obtained at a Pt–Mo RRDE in the same electrolyte composition as above (ring potential set at 1.0 V). Under these conditions, the observed ring and disc responses were analogous to those obtained previously at a Au–Mo RRDE. Again, the range of ring potential available at the platinum electrode is extremely limited because of alloy formation with aluminium. Consequently, the electrode reaction kinetics cannot be altered in a way that may allow the detection of other soluble species. Although no additional mechanistic details could be obtained at the Pt–Mo RRDE, the results support the reaction mechanism (Scheme 1) proposed above.

It has previously been established that aluminium can form an alloy with the disc substrate material [19]. Figure 4 shows a scanning electron micrograph of a molybdenum cathode after polarization in the cryolite–alumina electrolyte at $1\,A\,cm^{-2}$ for approximately 60 min at 975 °C. Energy dispersive and wavelength dispersive spectroscopy revealed the existence of a primary and a secondary Mo–Al rich phase

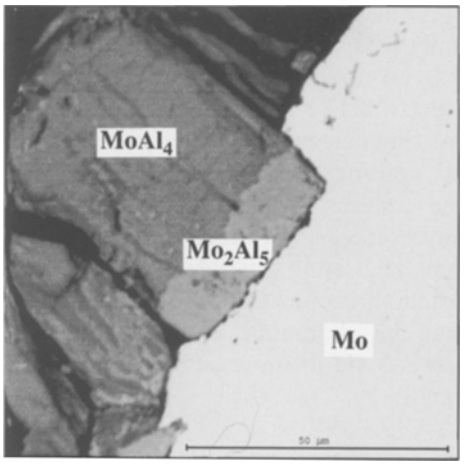

Fig. 4. Scanning electron micrograph using back-scattered electron imaging of a cross-section of a molybdenum cathode following cathodic polarization in an electrolyte of 90 wt % cryolite and 10 wt % alumina at $1\,A\,cm^{-2}$ for ~ 60 min at 975 °C (bar = 50 μm).

resulting from alloy formation; these were identified as $MoAl_4$ and Mo_2Al_5 (rather than the recognized phase $MoAl_3$ [23]), respectively. It is concluded that both of these alloys are formed as a result of the dissolution of molybdenum into the aluminium deposit produced during long-term electrolysis. In view of the above, it may also be necessary to consider the implications of alloy formation on the overall reaction mechanism for aluminium electrodeposition. An alternative scheme, involving the formation of an aluminium alloy, can also be written:

Step 1: alloy formation

Disc:

$$Al(III)_{(melt)} \xrightarrow{3e^-} Al(0)_{(alloy)} \rightleftharpoons Al(0)_{(dissolved)}$$

$$\downarrow -3e^-$$

Ring: $Al(III)_{(melt)}$

Step 2: bulk deposition

Disc:

$$Al(III)_{(melt)} \xrightarrow{3e^-} Al(0)_{(liquid)} \rightleftharpoons Al(0)_{(dissolved)}$$

$$\downarrow -3e^-$$

Ring: $Al(III)_{(melt)}$

Scheme 2

The main difference between the mechanisms presented in Schemes 1 and 2 is whether the reaction proceeds via the formation of a subvalent intermediate species or, in two steps, via an aluminium alloy. The first and second oxidation waves at the ring are consistent with the formation of aluminium at a reduced activity in an alloy and at unit activity, respectively. It is difficult to differentiate between Schemes 1 and 2 since one would expect both Al(I) and $Al(0)_{(alloy)}$ to be formed at potentials less negative than that required for formation of $Al(0)_{(liquid)}$. However, the disc currents for the first oxidation process at the ring, are much larger than those observed previously for alloy formation [19]. This strongly suggests that the observed ring response arises from the detection of species generated from

bulk aluminium electrodeposition and not alloy formation.

Scanning electron microscopy was also used to examine the surface of a Au–Mo RRDE after it had been cathodically polarized at −0.2 V for 1 min in an electrolyte consisting of 90 wt % cryolite and 10 wt % alumina at 975 °C ($BR = 1.5$). These investigations revealed no evidence of interdiffusion between deposited aluminium and the molybdenum electrode surface, suggesting limited interaction on the timescale of an RRDE experiment. These results tend to confirm that alloy formation does not significantly interfere with electrochemical measurements of the aluminium electrodeposition process. Therefore, a reaction sequence involving both the formation of a subvalent intermediate species and the chemical dissolution of aluminium metal, via Scheme 1, appears to be the most probable pathway.

3.2. *Influence of electrolyte composition on reaction mechanism*

Since it is possible that electrolyte composition could significantly affect the electrochemical responses obtained at an RRDE, further investigations were conducted in an electrolyte approaching that commonly employed in industrial operations. Figure 5 shows current–voltage curves obtained at a Au–Mo RRDE in an electrolyte of 75.7 wt % cryolite, 4 wt % alumina, 15.3 wt % aluminium fluoride and 5 wt % calcium fluoride ($BR = 1.0$) at 945 °C, as a result of scanning the disc potential in the negative direction while maintaining the ring potential at 1.2 V. As was observed above, the disc current–disc potential curves were again characterised by a large single cathodic wave, attributed to the reduction of Al(III) to Al(0), irrespective of whether measurements were made at a stationary or rotating RRDE. At a rotation rate of 1000 r.p.m., two well defined oxidation waves were again observed at the gold ring, as shown by the ring current–disc potential curve. In this case a peaked maximum was observed for the second oxidation process which has so far not been satisfactorily interpreted, although it may be related to the expected reduction in Al(0) solubility, caused by the addition of aluminium fluoride which lowers the BR of the electrolyte. Generally, this type of behaviour was observed in other electrolyte compositions examined ($BR \leq 1.0$), where aluminium fluoride was employed at levels in excess of 15 wt %.

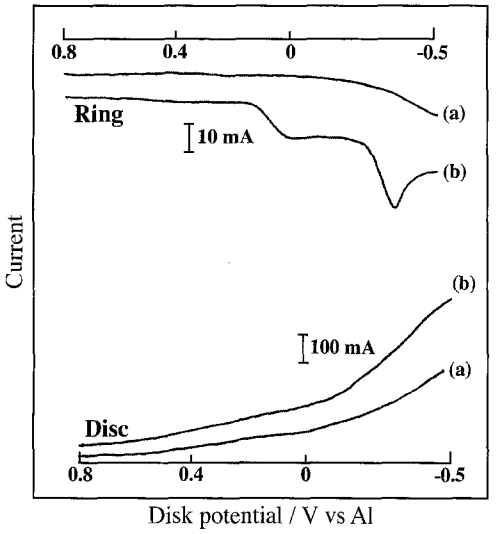

Fig. 5. Typical disc current–disc potential and ring current–disc potential curves obtained at a Au–Mo RRDE ($r_1 = 0.50$ cm, $r_2 = 0.54$ cm, $r_3 = 0.64$ cm, disc area = 0.79 cm^2, and ring area = 0.37 cm^2) in an electrolyte of 75.7 wt % cryolite, 4 wt % alumina, 15.3 wt % aluminium fluoride and 5 wt % calcium fluoride at 945°C ($BR = 1.0$). (a) Stationary electrode, ring potential 1.2 V and potential scan rate 50 mV s^{-1}. (b) Rotation rate 1500 r.p.m., ring potential 1.2 V and potential scan rate 50 mV s^{-1}. (Bottom and top abscissae: disc and ring currents zero, respectively.)

The electrochemical responses obtained at the Au–Mo and Pt–Mo RRDEs were more difficult to characterize in lower temperature electrolytes (≤ 900 °C). In some instances, only a single poorly defined oxidation wave was observed at the ring. This implies either that the aluminium electrodeposition process does not proceed via an intermediate, or alternatively, that an intermediate with a very short half-life is involved in the reaction mechanism. This apparent variation in electrochemical behaviour may also be due to factors additional to changes in electrolyte properties, for example, phenomena associated with electrode passivation. The influence of electrolyte composition on the aluminium electrodeposition process is an area that is not well understood and clearly warrants further investigation. In this sense, our findings should be considered as a qualitative assessment of the type of behaviour occurring in lower temperature electrolytes. Nevertheless, the above results do indicate that the faradaic responses obtained at an RRDE are dependent upon the electrolyte composition.

4. Conclusions

The present work demonstrates that a high temperature RRDE can be used to obtain important electrochemical data in cryolite-based electrolytes. An investigation of the aluminium electrodeposition process using the RRDE technique has shown that the reaction proceeds via a multi-step mechanism involving two discrete electron-transfer steps coupled to a chemical reaction step. Most importantly, it is shown that under certain conditions it is possible to detect a subvalent intermediate species Al(I). The proposed overall reaction mechanism (Scheme 1) confirms present hypotheses that chemical dissolution of Al(0) into the bulk electrolyte is primarily responsible for the loss in current efficiency in aluminium smelting cells. Since the rate of the Al(I) to Al(0) reaction increases with current density, the formation of a subvalent intermediate species is unlikely to significantly influence the current efficiency at the high current densities employed in industrial operations (~ 0.8 A cm^{-2}). However, it could be expected that in regions of low current density and high mass transfer rates, such as at the cathode-ledge areas, locally low current efficiencies could be experienced.

Acknowledgements

The authors gratefully acknowledge the technical assistance of J. F. Kubacki for the skilful construction of the various high temperature rotating ring-disc electrodes, and P. Rummel and C. M. MacRae for assistance and advice on the scanning electron microscopy investigations. We also thank S. Fletcher, W. H. Kruesi and R. Woods for comments on the manuscript, and A. M. Vecchio-Sadus for advice on electrolyte composition and preparation. We acknowledge Comalco Research Centre, Victoria, Australia for the supply of electrolyte materials.

References

[1] J. P. Saget, V. Plichon and J. Badoz-Lambling, *Electrochim. Acta* **20** (1975) 825.
[2] E. W. Dewing and K. Yoshida, *Can. Met. Quart.* **15** (1976) 299.
[3] K. A. Bowman, Doctoral Dissertation, University of Tennessee, Knoxville, TN (1977).
[4] J. Thonstad and S. Rolseth, *Electrochim. Acta* **23** (1978) 223.
[5] J. J. Duruz, G. Stehle and D. Landolt, *ibid.* **26** (1981) 771.
[6] J. J. Duruz and D. Landolt, *J. Appl. Electrochem.* **15** (1985) 393.
[7] R. Ødegard, *Electrochim. Acta* **33** (1988) 527.
[8] E. Y. L. Sum and M. Skyllas-Kazacos, *J. Appl. Electrochem.* **18** (1988) 731.
[9] *Idem, Electrochim. Acta* **36** (1991) 31.
[10] J. J. Del Campo, J. P. Millet and M. Rolin, *ibid.* **26** (1981) 59.
[11] J. M. Tellenbach and D. Landolt, *ibid.* **33** (1988) 221.
[12] J. W. Burgman and P. J. Sides, *ibid.* **34** (1989) 841.
[13] E. W. Dewing, *Can. Met. Quart.* **30** (1991) 153.
[14] R. M. Wightman and D. O. Wipf, *Acc. Chem. Res.* **23** (1990) 64.
[15] B. Malinowska, M. Cassir and J. Devynck, *J. Electrochem. Soc.* **141** (1994) 2015.
[16] W. J. Albery and M. L. Hitchman, 'Ring-Disc Electrodes', Oxford University Press, Oxford (1971).
[17] F. Opekar and P. Beran, *J. Electroanal. Chem. Interf. Electrochem.* **69** (1976) 1.
[18] S. Bruckenstein and B. Miller, *Acc. Chem. Res.* **10** (1977) 54.
[19] R. S. Stojanovic, J. F. Kubacki, R. Dorin and E. J. Frazer, *J. Appl. Electrochem.* **25** (1995) 456.
[20] J. W. Burgman, J. A. Leistra and P. J. Sides, *J. Electrochem. Soc.* **133** (1986) 496.
[21] E. J. Frazer and I. C. Hamilton, *J. Appl. Electrochem.* **16** (1986) 387.
[22] A. Damjanovic, M. A. Genshaw and J. O'M. Bockris, *J. Chem. Phys.* **45** (1966) 4057.
[23] M. Hansen and K. Anderko, 'Constitution of Binary Alloys', 2nd edn, McGraw-Hill, New York (1958).